ORIGINAL ARTICLE

Failure modes classification and failure mechanism research of ancient city wall

Guoqing Chen[1] · Le Li[1] · GuangMing Li[1] · XiangJun Pei[1]

Abstract
Many ancient city walls have stability problems such as internal damage, surface weathering and erosion, and even degradation of bearing capacity. The protection of ancient city wall has thus become a serious problem to be solved, and this study was carried out to provide specific protection recommendations. We identified and classified the failure modes of a number of ancient city walls and give specific protection recommendations for different kinds of failure modes. Based on numerical simulation, the analysis of the failure mechanism of an ancient city wall in Beijing has put forward. We found that the main failure mode of ancient city wall is rainstorms and that the rainfall degree, the duration of rainfall, and the presence of permeable channels in the wall all have a significant impact on the deformation of the wall, and there may have a bulging phenomenon in the lower part of the surface of the wall; in addition, the temperature has little effect on the deformation of the wall. Our classification method can be applied to identify the failure modes of similar ancient buildings and can provide suggestions for protective measures.

Introduction

City walls, built as fortifications in ancient times, have become unique historical cultural monuments. However, after a long period of rainfall erosion, hidden weak spots were developed, such as small holes or micro-cracks inside the walls, which can lead to their collapse (Fabio et al. 2015; Dina and Sara 2011). The importance of the protection of historical cultural heritage urges to carry out the renovation of the ancient city walls. As historical information about damage of ancient city walls is not available, it is difficult to judge the degree of destabilization of the whole structure and its ability to resist further deformation. A number of studies have contributed to new knowledge about city wall protection. The influence of weathering on the ancient city wall is illustrated by Kamh (2011), who studied the weathering, and bio-deterioration and the rate of weathering

were measured with MEM (micro-erosion meter) equipment in Aachen City (Kamh and Serdar 2016). The influence of vegetation (Li et al. 2016) and the natural environmental conditions (Xu et al. 2016) on wall damage makes clear that the deterioration by these natural factors should be addressed as early as possible.

In order to understand the mechanism of wall failure, numerical simulations (Ronnie and Yossef 2008; Wu et al. 2013) were carried out. The deformation characteristics of city walls due to their own weight, continuous rainfall, and seismic loading are analyzed by FLAC3D, and we concluded that the plastic deformation is most likely to occur at the junction of the walls and the foundation ground, and at the contact of the walls with the compacted earth (Li and Zhang 2015). Meanwhile, analytical investigations techniques for stone blocks were developed (Bolognesi et al. 2004; Liu et al. 2016; Xiao et al. 2014). A large variety of monitoring equipment such as LIDAR and scanning electron microscope has been used in the protection of the ancient city wall, to not only monitor the deformation but also identify weak points, evaluate the overall stability, and provide early warning for failures (Fabio et al. 2014, 2015; Timothy et al.

✉ Guoqing Chen
  chgq1982@126.com

[1] State Key Laboratory of Geohazard Prevention and Geoenvironment Protection, Chengdu University of Technology, Chengdu 610059, Sichuan, China

2014; Deodato et al. 2013; Wang et al. 2013; Liu et al. 2016; Tsokas et al. 2011).

This means that fruitful research has already been carried out on the monitoring of failure and deformation of ancient city walls, but the understanding of the failure mechanism and failure mode of such walls is still inadequate. Therefore, the aim of our research was to understand the mechanism of wall failure and to make a classification of the failure modes.

We present a failure mode classification which can be used as a reference for the construction personnel to design measures for the protection and treatment of ancient city walls. A case study is presented in which the failure mode of an ancient city wall is discussed.

Failure modes classification

Based on a review of the existing literature about the research on failure modes of ancient walls, we classified the failure modes into failures controlled by "natural factors" and those controlled by "structural factors." These control factors can be refined to specific failure factors such as rainfall, extreme climate, bulging, potential sliding surfaces, and so on. In fact, a city wall failure is often caused by a combination of various failure factors. Originally, protection engineering was not based on the failure factors but on the types of diseases by taking the corresponding protective measures. Based on this theory, the classification of failure modes was based on the types of diseases. Since there may be many different deformation mechanisms caused by the same disease type such as weathering and crack propagation, the tertiary classification of failure modes was developed, based on the observed phenomenon. We defined 12 kinds of typical phenomena, as shown in Fig. 1.

"Natural factor control" phenomena are due to long-term climatic effects such as heavy rain, strong wind, extreme cold, which can cause failures such as cracking, bulging, swelling, and instability. "Structural factor control" phenomena are related with small holes, cracks, or potential structural planes as the dominant factor of controlling the deformation degree from the city wall.
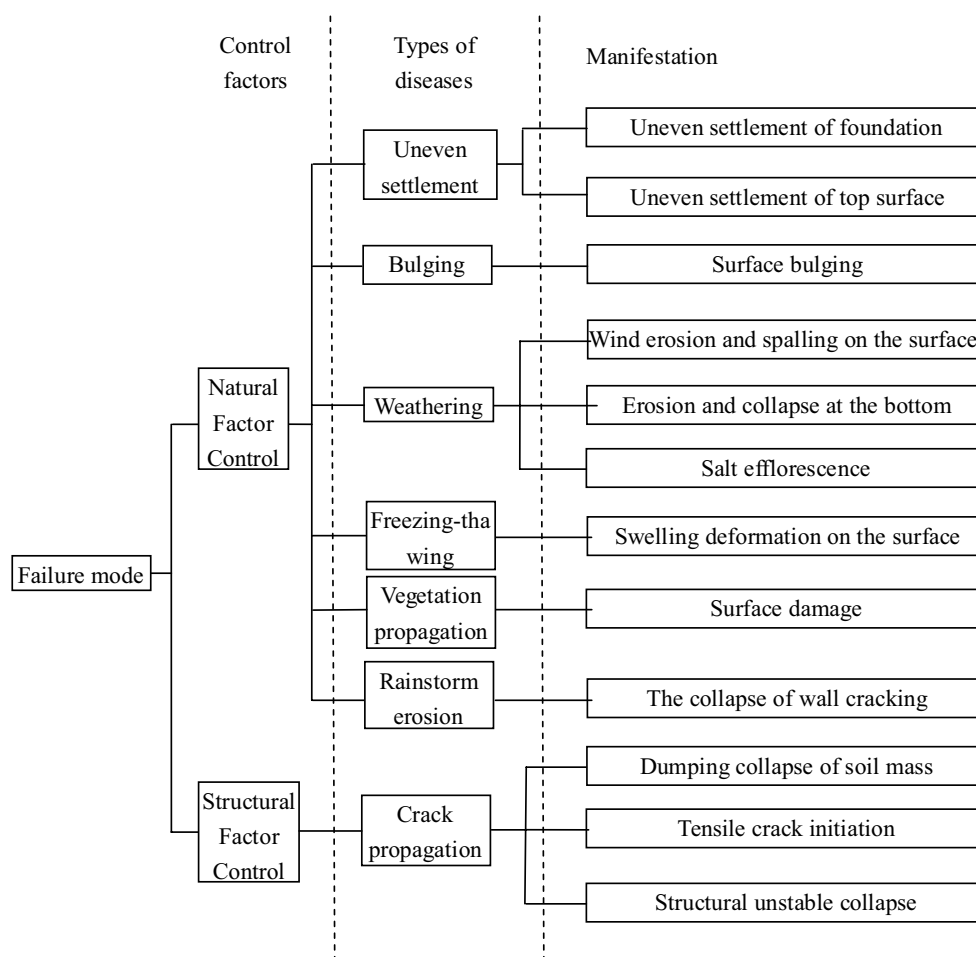
Fig. 1 Our newly developed wall failure modes classification system

It should be noted that there is usually not one single controlling factor in a certain failure mode. For example, the main controlling factor of freezing–thawing is the external temperature, but there are also cracks initialing and bulging inside the wall, which has a little impact on the deformation. In general, the failures of city walls consisting of soil are mainly controlled by natural factors, but after the internal cracks in the soil have widened, the failure is mainly controlled by crack development, which is less controlled by the natural factors.

Table 1 gives a detailed presentation, which includes the forms of diseases, failure mechanisms, occurrence location, and protective measures for different failure modes. Schematic diagrams of the failure modes and characteristic photographs are also included, which is convenient for field monitoring and construction personnel to identify the failure mode and to predict the failure process [some pictures refer to the following paper or thesis (Cao et al. 2013; Ao and Ying-yang 2008)]. Based on the basic physical properties, chemical composition, and natural environment of the ancient city walls, rational methods of analysis and suggestions for protective measures are adopted to prevent and control wall failures, which make the classification system more practical.

Failure mode recognition and numerical analysis: taking the city wall in Beijing for an example

Problem analysis

Due to long-term erosion and adverse human activities, the city wall located in Beijing had suffered huge load fluctuations, which have caused leakage into the wall body through the bricks on the surface, uneven settlement, and spalling at the wall surface.

The state of damage is shown in Figs. 2 and 3. There are cracks at the foot of the wall with brick dislocation phenomena (Fig. 2), which indicate that there may have been uneven settlement of the foundation, and we observed bulging; therefore, the damage of the wall is probably caused by these two failure modes. Figure 3 shows the leakage of water at the foot of the wall, which indicates that there are cracks filled with water inside the wall. If the water cannot be discharged in time, the internal cracks will widen, which may cause spalling at the wall surface or even collapse.

Drill hole sampling has shown that the core of the wall was completely composed of brick masonry and there is no compacted soil inside; therefore, the possibility of differential soil settlement and the occurrence of potential sliding surfaces can be eliminated. Based on our new failure mode classification system (Table 1), in combination with the monitoring report and other relevant geological survey data, we concluded that the key factors of the wall damage are rainstorm erosion and uneven settlement due to infiltration and seepage. The effect of climate change on wall deformation is not clear since the bulging phenomenon may be caused by freezing–thawing, which needs further discussion.

Analysis of city wall damage

Based on the results of the field survey, the key factor of the wall damage is rainstorm erosion as the effect of climate change on wall deformation is not clear since it may cause brick dislocation phenomena. The finite element analysis software FLAC3D was used to identify the main controlling factors of wall failure and reveal the deformation behavior of the wall under different loading conditions (Itasca Consulting Group 2003). In this study, heavy rainfall and long-term temperature effects are analyzed by using FLAC3D to evaluate the stability of the wall. During the finite element calculation, the Mohr–Coulomb model is used for the ground material failure, including uneven settlement, crack initiation, and other structural damage factors. The general principle is shown in the following (Eq. 1):

$$\tau_f = \sigma \times \tan\varphi + c, \tag{1}$$

where c is the cohesion (kPa), φ is the friction angle (°), σ is the stress value (kPa), and τ_f is the shear strength (kPa). The Mohr–Coulomb strength criterion can identify the plastic zones, which indicate the most vulnerable areas so that we can decide where to carry out protection works.

Heavy rainfall analysis

The finite element numerical software can simulate the fluid flow inside the wall. In the seepage model, transient seepage calculation and fluid–solid coupling calculations are carried out. The change in pore water pressure will lead to mechanical deformation so that the most vulnerable areas during rainfall can be identified. The rainstorm erosion problem of city walls can be modeled with the Darcy's Law, which is used for the seepage failure, including the rainstorm erosion. The general principle is shown in the following (Eqs. 2 and 3):

$$Q = KAJ = KA\frac{H_1 - H_2}{L} \tag{2}$$

$$V = \frac{Q}{A} = KJ, \tag{3}$$

where Q is the seepage discharge through the cross section (m^3/s), K is the permeability coefficient of the porous media (m/s), A is the cross-sectional area (m^2), H_1 and H_2 are the hydraulic heads upstream and downstream in the cross
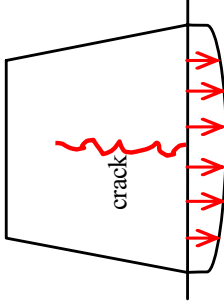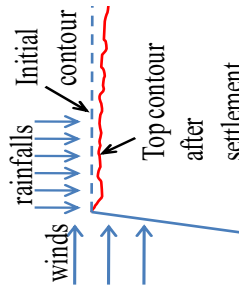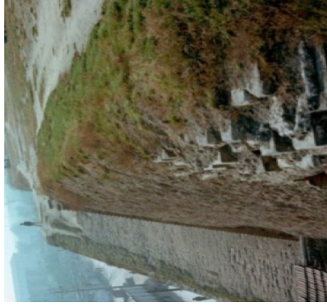
Table 1 Classification of wall failure modes

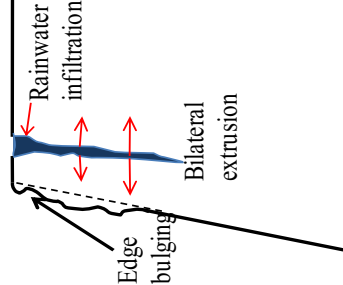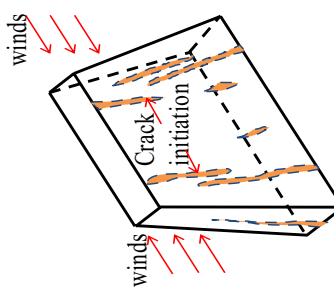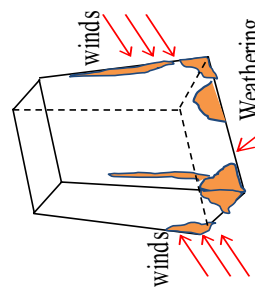| Failure mode			Failure mechanism	Occurrence location	Sketch map	Physical map	Protective measures suggestions
Main class	Subclass	Manifestation					
Natural factor control	Uneven settlement	Uneven settlement of foundation	Affected by rainfall and human activities, the strength of soil around the foundation has decreased	Surrounding the foundation			Increase the density of the wall and restore the wall, monitor regularly
		Uneven settlement of top surface	Long-term natural effects or thermal reactions cause wall spalling, wind erosion, and other damages at the top surface	Top surfaces			Weatherproofing material is needed, make overall repair when necessary
	Bulging	Surface bulging near top of the wall	Heavy rainfall infiltrates into cracks and squeezes the soils, leads to a decrease of the shear and causes dilation	Surfaces of city wall			Repair the drainage system, fill the holes in the wall surface, and monitor regularly

Table 1 (continued)
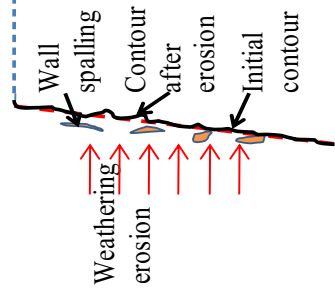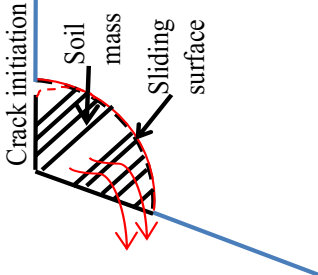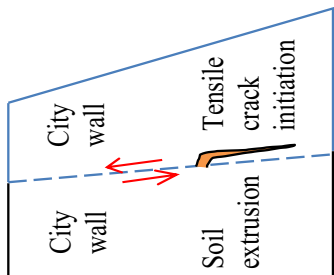
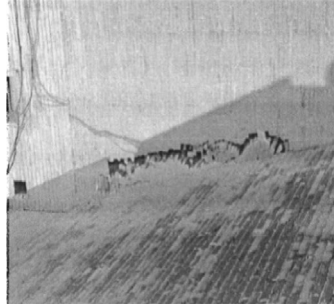| Failure mode			Failure mechanism	Occurrence location	Sketch map	Physical map	Protective measures suggestions
Main class	Subclass	Manifestation					
	Weathering	Wind erosion and spalling on the surfaces of the city wall	Weathering due to acid rain, corrosion, freezing, and crystallization of soluble salts leads to crack initiation	Surfaces of city wall			Increase the strength of the wall, surface protection materials are needed, do monitor regularly
		Erosion and collapse at the bottom	The stability of the wall decreases due to the effect of wind erosion at the bottom of the foundation	At the bottom of the wall			Revamping the foundation, apply surface protection materials
		Salt efflorescence at the surface	Alkali and salt dissolved in the building materials are crystallized on the surface of the wall, which leads to the spalling of the surface	Surface of the wall			Strip the surface, replace damaged bricks, and use alkali-removing agent

Table 1 (continued)
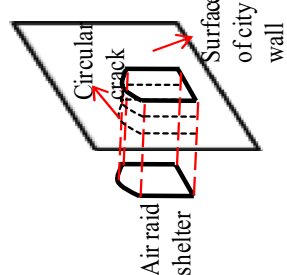
Failure mode			Failure mechanism	Occurrence location	Sketch map	Physical map	Protective measures suggestions
Main class	Subclass	Manifestation					
	Freezing–thawing	Swelling deformation on the surfaces of the city wall	Temperature differences, crack initiation, and heavy rainfall increase the porosity and decrease the strength of the soil, which leads to cracks and bulges	Top surfaces, inside the wall, and at the bottom of the foundation	Frost heave melting / Crack initiation / Wall expansion		Cover the wall with cement grout, anti freezing–thawing materials are needed, take insulation measures when necessary
	Vegetation propagation	Surface damage on the surfaces of city wall	Vegetation development is flourishing, which destroys the overall stability of the wall, leading to the collapse of the wall	Surfaces of city wall	Roots development / Vegetation growth		The vegetation should be removed as far as possible and be monitored regularly
	Rainstorm erosion	The collapse of wall cracking	Continuous heavy rain is not properly discharged, which causes the porosity to increase and causes crack initiation and bulging	Surfaces of city wall	Rainfalls / Crack infiltration / Rainwater infiltration surface		Repair the drainage system, increase the compactness of the wall, and take anti-infiltration measures

Table 1 (continued)

Failure mode			Failure mechanism	Occurrence location	Sketch map	Physical map	Protective measures suggestions
Main class	Subclass	Manifestation					
Structural factor control	Crack propagation	Sliding collapse of soil mass	The micro-cracks expand unceasingly, which leads to the formation of a sliding surface and to slip failure	Surface of city wall			Improve the sealing treatment of the top of the wall (install anchors), and monitor regularly
		Tensile crack initiation	Differential settlement between the old and the new soils leads to the cracks and collapses	At the junction of the wall and the joint between the city walls			Repair the cracks, increase the density and the connection between the junctions of the wall
		Structural unstable collapse	Thermal expansion and contraction cause cracking inside the chamber, which may affect the overall strength of the wall and cause collapse	Chamber inside the wall or air raid shelter			Working on the cement grouting, filling treating of cracks

Fig. 2 Brick dislocation of ancient wall

section (m), *L* is the infiltration path (m), *J* is the hydraulic gradient, which means the hydraulic head loss per unit length along the seepage path, and *V* is the seepage velocity (m/s). In the simulation process of heavy rainfall, the hydraulic gradient can be controlled by controlling the seepage discharge to obtain the most realistic results.

The numerical model is a cross section with a thickness of 0.9 m and with the same size as the city wall (36.8 m × 12.96 m). The wall model is regarded as an isotropic fluid model not taking into account the compressibility of soil. In order to fit with the actual rainfall situation, the mechanical parameters are determined by combining the results of direct shear tests of field samples. Drill hole sampling has shown that the core of the wall was completely composed of brick masonry; therefore, the city wall can be

considered as homogeneous material. The best fitting seepage parameters were selected after several physical model tests, considering the basic physical properties and natural environment of the city walls, as shown in Table 2.

The rainfall process is simulated by applying the rainfall on the surface of the wall and setting the ground water discharge boundary at the lower surface of the wall. The bottom surface and both sides of the city wall are fixed in the model. The objective of the simulation is to determine the influence of rainfall intensity on the failure of the wall. Five reference points located at the surface of the city wall are selected to monitor the increasing displacement in the x direction and the development of a plastic zone (Fig. 4). The simulation started with the rainfall on top of the wall, while the groundwater seepage was limited at the surfaces of the wall. Rainfall intensities of 10, 20, 30, and 40 mm/h were simulated for 24 h, while the deformation trend and the formation of a plastic zone were studied (Figs. 5 and 6).

Figure 5 shows the deformation trend in the horizontal direction of each reference point on the surface of the wall model, which is mainly concentrated on the lower part of the surface of the wall (Points 2–4), while the deformation at the top (Point 1) and the bottom (Point 5) is small. With the increase in rainfall intensity, the displacements in the horizontal direction increase with a linear growth trend, which indicates that the deformation of the wall is related to the rainfall intensity.

The formation of a plastic zone under different rainfall intensities is shown in Fig. 6. When the rainfall intensity is small (10, 20 mm/h), the rainwater which is accumulated in the cracks and holes can be discharged in time, and

Fig. 3 Seepage and cracks at the foot of the wall

Table 2 Mechanical parameters and seepage parameters of ancient city wall

Elastic modulus E (MPa)	Poisson ratio *u*	Cohesion c(KPa)	Internal friction angle φ (°)	porosity	Permeability coefficient (m/s)	Fluid density (kg/m^3)	Fluid tensile strength	Fluid modulus (MPa)	Saturation level
700	0.1	300	36	0.1	1e−10	1000	1e−12	2e4	0.05

Fig. 4 Finite element model of the wall and the position of the reference points
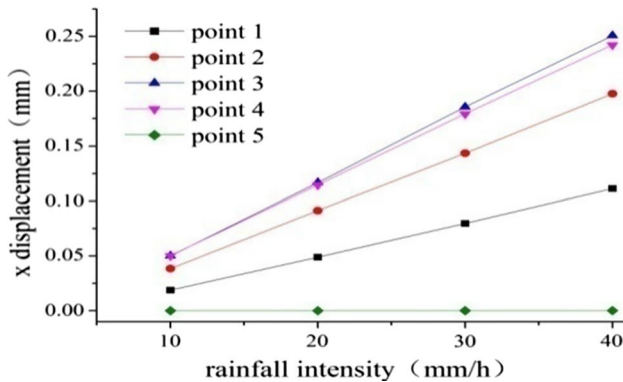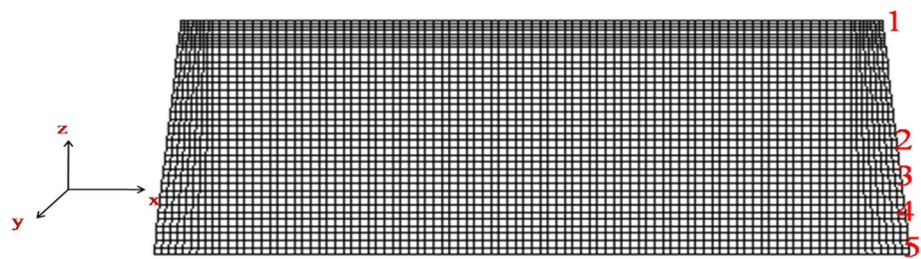
Fig. 5 Trend of the horizontal displacements of the reference points

plastic failure is not developed. As the rainfall intensity increases, the rainwater cannot be discharged in time and cracks and holes are filled with water, the plastic failures occurred (black area) which leads to crack widening and water leakage.

In order to obtain more detailed information about behavior of the wall under strong rainfall conditions, we applied repeated continuous heavy rainfall during the numerical model testing. The applied rainfall intensity was 40 mm/h, during two rainstorms with an interval of 1 day. Figure 7 shows the displacements of the reference points in the horizontal direction. After the two rainstorms, the displacements in the horizontal direction are still concentrated on the middle and lower part of the surface of the wall. The maximum displacement is about 0.7 mm (Fig. 7), which is more than twice as much as after a single heavy rainfall (0.25 mm). A comparison with the deformations after a single rainstorm shows that the failure affected areas were expanded at the surface of the wall. After continuous and repeated heavy rain, the wall cracks widened and plastic failures appeared in the middle and lower part of the wall surface (Fig. 8), visible as a local convex bulging phenomenon shown in Fig. 9.

The observed behavior can cause the collapse of the city wall. Therefore, to prevent such problems, surface protection materials should be applied on the wall and real-time monitoring should be proposed regularly; meanwhile, the permeable channel at the top of the wall should be improved and anti-infiltration measures should be taken.

Long-term temperature effects

The influence of temperature changes on the deformation of the city wall is mainly occurring as the damage caused by freezing and thawing. By using FLAC3D, the thermo-mechanical coupling model can simulate the transient heat conduction in the material, leading to displacements and stresses. The applicable thermal equations are used for the failure modes, including bulging and the freezing–thawing. The applicable energy equations are Eqs. (4) and (5):

$$-q_{i,j} + q_v = \rho C_v \frac{\partial T}{\partial t}, \tag{4}$$

$$\Delta \sigma_{ij} = -3\alpha K \delta_{ij} \Delta T, \tag{5}$$

where q_i is the heat flux vector (W/m^2), q_v is the body heat source intensity (W/m^3), ρ is the density, C_v is the amount of heat in a certain volume [J/(kg K)], T is the temperature (°C), t is the time (s). α is the thermal expansion coefficient (K^{-1}), K is the bulk modulus (kPa), δ_{ij} is the Kronecker symbol, ΔT is the amount of temperature change (°C), and $\Delta \sigma_{ij}$ is the change in stress caused by temperature (kPa). In the thermal simulation, by using Eqs. (4) and (5), the internal stress of the city wall is only controlled by the temperature fluctuations, which makes the simulation process more simple and concise.

The thermo-mechanical coupling model is consistent with the seepage model and can be considered as anisotropic thermal model. When selecting the thermal parameters, the thermal parameters of a similar brick masonry wall were used, combined with the monitored temperatures by taking the comprehensive thermal value. These are based on the average temperature and the minimum temperature of each season in Beijing and are shown in Tables 3 and 4.

In order to make the internal temperature field match with the actual situation, the bottom surface of the wall was designed that no heat could leak out of the bottom and the temperature was set on the surfaces of the wall. The bottom and both surface sides of the city wall are fixed. The objective of the simulation is to determine the influence of temperature fluctuations on the failure of the wall in two different climatic conditions. Fourteen reference points on the top and the right-hand surface of the model were selected

Fig. 6 Development of plastic zones at different rainfall intensities. **a** 10 mm/h, **b** 20 mm/h, **c** 30 mm/h

(a)

(b)

(c)

(d)
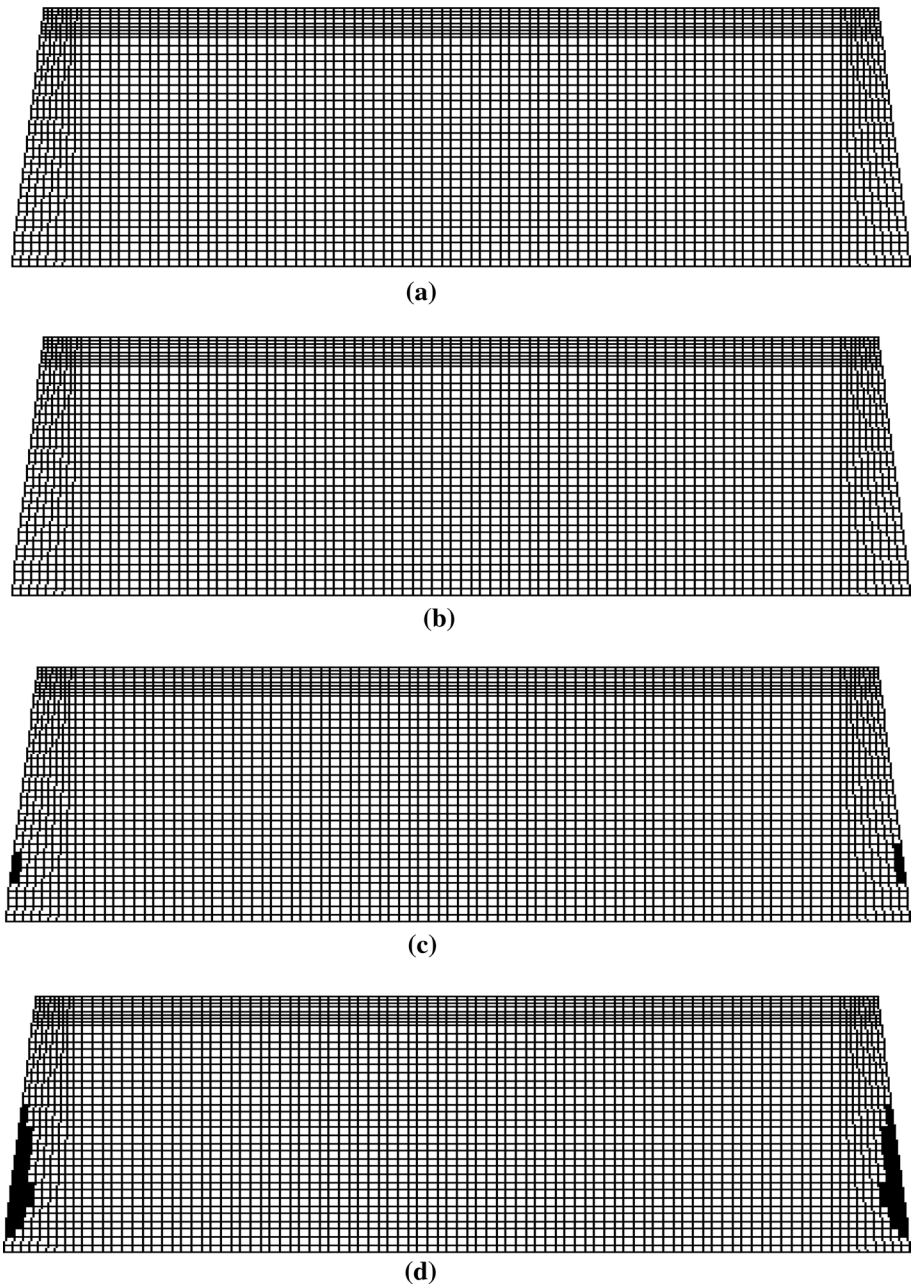
Fig. 7 X displacement distribution after two heavy rainstorms
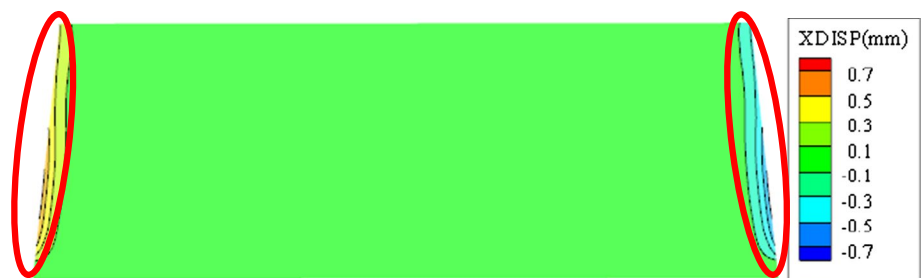
(Fig. 10) to monitor the deformation of the city wall. The simulation started with the fluctuation of the temperature, with a 20 years cycle from spring to winter.

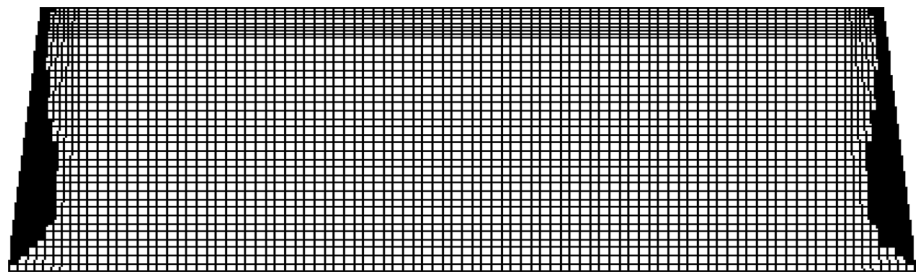Figure 11 shows the deformation in the X (horizontal) and Z (vertical) directions of the city wall under average climatic conditions for a period of 20 years. It shows that

Fig. 8 Plastic zones formed after two heavy rainstorms

Fig. 9 Local bulging of ancient wall

Table 3 Thermal parameters of city wall

Thermal conductivity [W/(m·K)]	Thermal expansion coefficient (K^{-1})	Specific heat [J/(kg·K)]
0.69	9.5e−6	750

Table 4 Monitoring temperature in each season (unit: °C)

|	Spring	Summer	Autumn	Winter
Normal climate	6	23	18	0
Extreme cold climate	1	18	15	− 5

under the influence of thermal expansion and contraction, the settlement was mainly concentrated on the top surface with a maximum settlement of 0.5 mm in the 20th year, which is controllable. In the horizontal direction, the model has a symmetrical deformation pattern, with a maximum deformation of 0.5 mm, at both sides of the city wall. It can

be concluded that the settlement is small and will not cause large deformations, indicating that the overall stability of the wall is good under the influence of temperature fluctuations.

Figure 12 shows the deformation trend under average climatic conditions for a period of 20 years. With the changes in temperature, the wall undergoes thermal expansion and contraction. It can be concluded that after the temperature has reached a minimum and begins to rise again, the wall bulging deformation occurs at the top of the wall surface, while the wall begins to shrink inward when the temperatures fall. In the horizontal direction, Point 8, which is located at the top of the wall, shows the largest displacement, while point 14, which is located at the bottom of the wall, has the minimum deformation; in the vertical direction, there is no clear difference between the monitoring points and the maximum settlement is about 0.6 mm. During the initial stages of the simulation, the deformation increases greatly. After a simulation time of 10 years, the annual deformation amplitude decreases gradually and becomes stable, with a range of variation of not more than 0.3 mm. This can be explained by the fact that the initial temperature field in the wall was not yet stabilized, which causes the deformation to vary strongly. After the internal temperature field has stabilized, the influence of the temperature field on the deformation has also been eliminated. Therefore, under the premise of a stable temperature field inside the wall, the settlement fluctuates in a smaller range and the wall will not be damaged.

Figure 13 shows the deformation trend of all monitoring points under extreme cold weather conditions. In comparison, the maximum displacement in horizontal and vertical directions under extreme weather conditions (1.3 mm) is more than twice as much as the maximum displacement value (0.5 mm) under normal climatic conditions. Figure 13 also shows that the deformation trend over longer periods of time in an extreme climate is comparable to that under a normal climate, which indicates that the wall deformations remain in a controllable range. Thus, the conclusion can be made that the temperature has little impact on the city wall and the damage remains in controllable range.
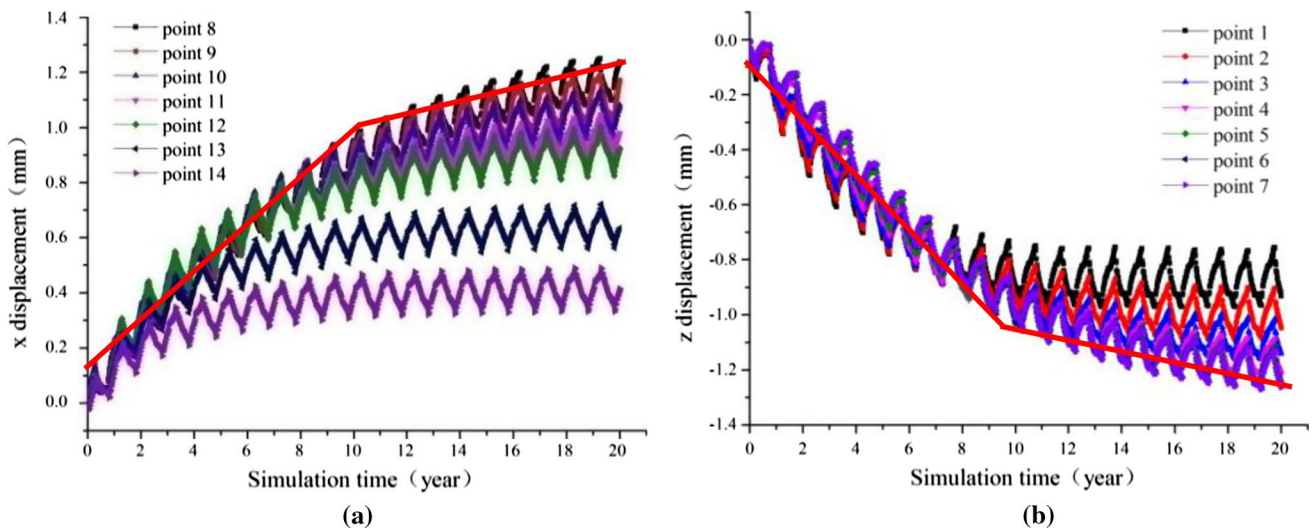
Fig. 10 Distribution of monitoring points on the thermomechanical model
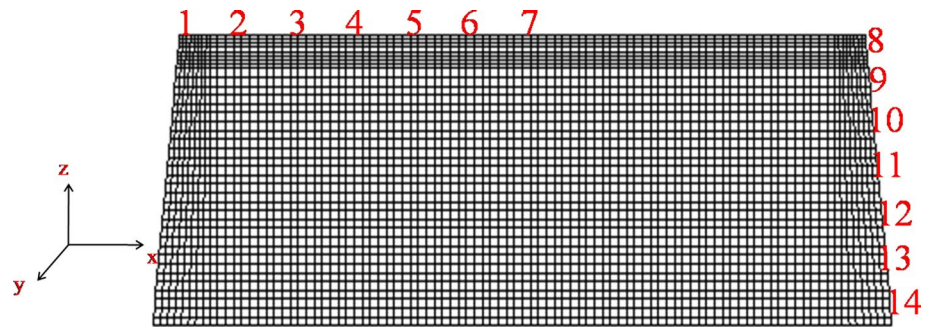
Fig. 11 Deformation of the wall under normal climatic conditions after 20 years
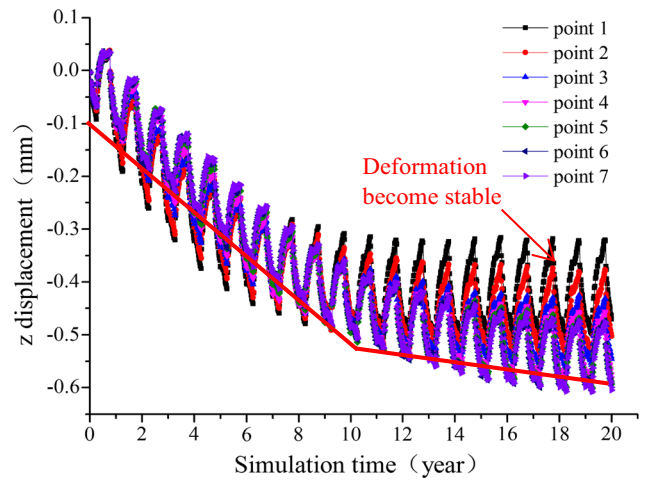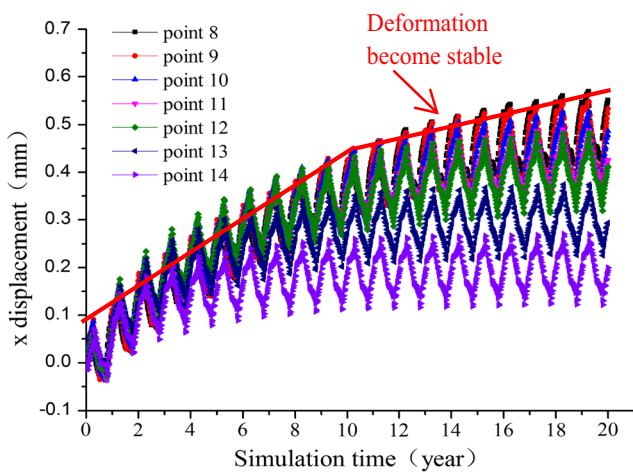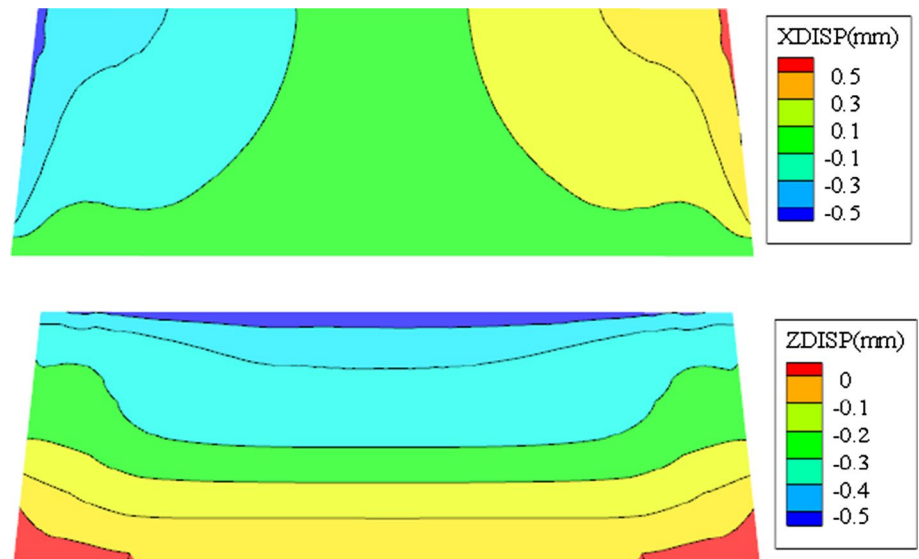
Fig. 12 Trends of the displacements of all monitoring points under normal climatic conditions. **a** Horizontal displacement, **b** vertical displacement

Fig. 13 Trends of the displacements of the monitoring points under extreme climatic conditions. **a** Horizontal displacement, **b** vertical displacement

Discussion

In this paper, aiming at the situation that the precursor information of ancient city wall was not clear and the protection work was difficult to carry out, the new city wall failure modes classification system was carried out. The following problems were found during the analysis:

It is indicated that the plastic failure may occur in the middle and lower part of the wall, which is consistent with the results of the study on high-step rock slope rainfall research (Li et al. 2017; Fan et al. 2005; Wu et al. 2010). It was mentioned that the hydraulic action and softening action of crack water may cause the collapse of rock slope, which is also applicable to the ancient city wall. The cracks and holes in the ancient city wall will expand when rainstorms occur regularly and a potential sliding surface is formed, since the hydraulic and softening influence of crack water is present inside the wall, which may lead to the failure of city wall. Therefore, the real-time monitoring should be proposed regularly in the rainy seasons, and the surface protection materials should be applied on the wall. In fact, many ancient city walls are masonry-concrete structure, we only consider the deformation of the single material city wall under rainfall condition in this study, and the effects of mixed materials in the rainfall situation were not applied, which needs further discussion.

For the numerical calculation of the seepage flow, six fluid parameters were used: porosity, permeability coefficient, fluid modulus, fluid tensile strength, fluid density, and saturation. The result of calculation and analysis showed that the porosity was the most significant parameter among these parameters. For a rainfall with intensity of 40 mm/h and duration of 1 day, the effect of porosity on the plastic failure is shown in Table 5.

Table 5 shows that the plastic zone is mainly located at the surface of the city wall. With an increase in the porosity, the plastic zone decreases in thickness. It shows that when the porosity was less than a critical value, the plastic deformation was intensified and the crack expansion phenomenon is more serious. The permeable channels inside the city wall affect the wall stability. When the permeable channels are blocked or partially blocked, the overall porosity of

Table 5 Effect of porosity on the simulation results

Porosity	0.07	0.08	0.09	0.1	0.11
Plastic zone					
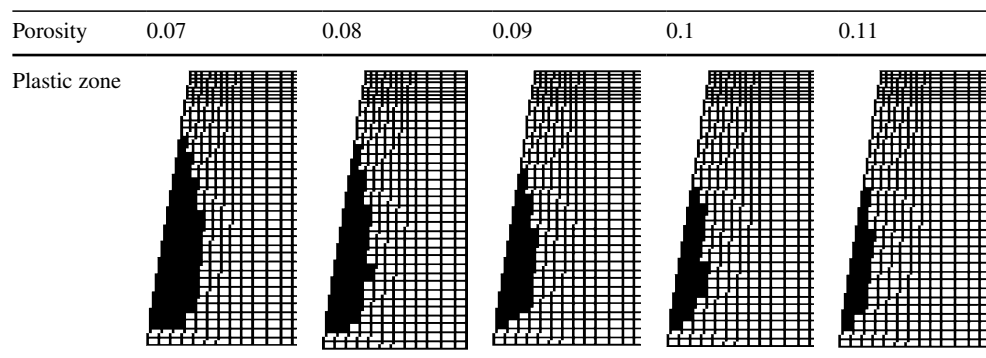
the whole city wall decreases and plastic failure may occur at the end of the wall due to rainfall, as shown in Table 5. Therefore, the permeable channels of the city wall must be kept clear to discharge the rainwater properly so that the city wall can be prevented from the heavy rainstorms failure.

In this paper, 12 typical failure modes were defined mainly based on the "control factors." In addition, there are other failure modes not determined by the "control factors"; they are mostly uncontrollable or unavoidable, such as earthquakes and incorrect human activities. When faced with such problems, the influences of this kind of failure should be eliminated as far as possible, in order to control the deformation of the city wall.

Conclusions

Our research of the failure modes of ancient city wall has led to the following conclusions:

1. Based on summarizing the domestic research results of the failure mode of ancient city wall, a complete classification system of the failure modes of ancient city wall is put forward, 12 typical forms can be distinguished, classified into three levels according to the "control factor," "disease type," and "occurrence location." The failure mechanism, schematic cross-section, and protective measures suggestions were described for each failure mode in Table 1, to provide as a reference for protection measures.

2. The city wall failure modes classification system was applied to an existing ancient city wall in China. First after field investigation and analysis of the failure mechanism, the failure mode was identified. Then, numerical simulation analysis confirmed that the main failure mode was rainstorm erosion. Rainstorm erosion can cause the plastic failure to act as bulging deformation as shown Fig. 9; therefore, deformation monitoring should be proposed in the rainy season to confirm the discharge of water. "Thermal expansion and contraction" due to the temperature fluctuation was found to be the main reason for the differential settlements of the city wall, which has a little impact on the city wall.

References

Ao Y-y (2008). Analysis of causes of cracks in the ancient city wall of Pingyao and the restoring measures. Beijing Jiaotong University. Master thesis. **(in chinese)**

Bolognesi E, Fabbri B, Macchiarola M et al (2004) Characterisation of historic bricks from the ruins of the great imperial palace in Istanbul. Key Eng Mater 264:2383–2386

Cao X-l, Li D-s, Liu W-h (2013) A survey of current status of the walls of the forbidden city and a preliminary exploration of its preservation. J Gugong Stud 01:342–353 **(in chinese)**

Deodato T, Nicola C, Guido L et al (2013) Integrating radar and laser-based remote sensing techniques for monitoring structural deformation of archaeological monuments. J Archaeol Sci 40(1):176–189

Dina FD', Sara P (2011) Assessment and analysis of damage in L'Aquila historic city centre after 6th April 2009. Bull Earthq Eng 9(1):81–104

Fabio B, Dario A, Domenica P et al (2014) A qualitative method for combining thermal imprints to emerging weak points of ancient wall structures by passive infrared thermography—a case study. J Cult Herit 15:199–202

Fabio P, Teresa N, Silvia B et al (2015) Early warning GBInSAR-based method for monitoring Volterra (Tuscany, Italy) City walls. IEEE J Sel Top Appl Earth Obs Remote Sens 8(4):1753–1762

Fan P, Liu Q-q, Li J-c et al (2005) Numerical analysis of rainfall infiltration in the slope with a fracture. Sci China Ser E Eng Mater Sci 48:107–120

Itasca Consulting Group Inc. (2003) Fast lagranginan analysis of continua in 3 dimensions, version 3.0, User's Manual [M]. Itasca Ltd., Minneapolis

Kamh GME (2011) Salt weathering, bio-deterioration and rate of weathering of dimensional sandstone in ancient buildings of Aachen City, Germany. Int J Water Resour Environ Eng 2(5):87–101

Kamh GME, Serdar K (2016) Micro-topographic and geotechnical investigations of sandstone wall on weathering progress, Aachen City, Germany, case study. Arab J Sci Eng 41:2285–2294

Li D-s, Zhang D (2015) Numerical simulation analysis of deformation of wall diseases of the Forbidden City. Tradit Chin Archit Gardens 3:62–65 **(in chinese)**

Li X-h, Yin X-m, Wang Y (2016) Diversity and ecology of vascular plants established on the extant world-longest ancient city wall of Nanjing, China. Urban For Urban Green 18:41–52

Li Z-q, Xue Y-g, Li S-c et al (2017) Deformation features and failure mechanism of steep rock slope under the mining activities and rainfall. J Mt Sci 14(1):31–45

Liu X-b, Ma X, Zhang B-j (2016) Analytical Investigations of traditional masonry mortars from Ancient City Walls built during ming and qing dynasties in China. Int J Archit Herit Conserv Anal Restor 10(5):663–673

Ronnie K, Yossef HH (2008) Numerical analysis of block stone displacements in ancient masonry structures: a new method to estimate historic ground motions. Int J Numer Anal Meth Geomech 32(11):1321–1340

Timothy H, Marilyn M, Bradley R (2014) High-DENSITY LiDAR mapping of the Ancient City of Mayapán. Remote Sens 6(9):9064–9085

Tsokas GN, Tsourlos PI, Vargemezis GN et al (2011) Using surface and cross-hole resistivity tomography in an urban environment: an example of imaging the foundations of the ancient wall in Thessaloniki, North Greece. Phys Chem Earth 36(16):1310–1317

Wang Y, Li E-b, Ge Z-z et al (2013) Monitoring and analysis of Ming Dynasty City wall safety influenced by construction of Jiuhuashan

tunnel. In: 2013 fifth conference on measuring technology and mechatronics automation

Wu Y, He S-m, Li X-p (2010) Mechanism of action of cracks water on rock landslide in rainfall. J Cent South Univ Technol 17:1383–1388

Wu C-f, Wang J, Zhang J-n (2013) Holistic analysis and restoration countermeasures on Ancient Great Wall of Shanhai Pass. Electron J Geotech Eng 18:4997–5010

Xiao Y, Fu X, Gu H-b et al (2014) Properties, characterization, and decay of sticky rice-lime mortars from the Wugang Ming dynasty city wall (China). Mater Charact 90:164–172

Xu H, Huang Q, Liu G et al (2016) A quantitative study of the climate-responsive design strategies of ancient timber-frame halls in northern China based on field measurements. Energy Build 133:306–320